Environ Monit Assess (2026) 198:558
https://doi.org/10.1007/s10661-026-15355-5

RESEARCH

Climate-driven distribution modeling of *Glossina fuscipes* (Diptera: Glossinidae) in the Afrotropical Region: current patterns, future projections, and implications for presence in the Arabian Peninsula

Magdi S. A. El-Hawagry · Rasha Al-Akeel · Abdulrhman Almadiy · Hathal M. Al Dhafer · Mustafa M. Soliman

Received: 6 August 2025 / Accepted: 18 April 2026

Abstract The tsetse fly *Glossina fuscipes* is the primary vector of human African trypanosomiasis (sleeping sickness) in Sub-Saharan Africa. While its distribution is confined to Africa, a 1990 report from Saudi Arabia created a long-standing biogeographical puzzle. We used MaxEnt species distribution modeling to project habitat suitability across the Afrotropical Region using 158 spatially filtered *G. fuscipes* occurrence records and bioclimatic variables generated from TerraClimate data (temperature and precipitation) for the reference period 1982–2023. Variables were selected using variance inflation factor analysis to minimize multicollinearity. Future projections employed an ensemble of five general circulation models under SSP1-2.6 and SSP5-8.5 scenarios for 2050 and 2070. The model demonstrated strong performance (training AUC = 0.940, test AUC = 0.931, TSS = 0.681). Precipitation of the driest period was the dominant predictor, followed by altitude, annual precipitation, and mean temperature of the driest quarter, emphasizing critical dependence on year-round moisture availability. Currently, *G. fuscipes* occupies 3.64 million km^2 (16.7% of Africa) concentrated in East and Central Africa. Climate projections reveal substantial expansion: 38–62% by 2050 and 47–95% by 2070, with minimal contraction (1.08–3.48%). Under SSP5-8.5, suitable habitat could nearly double by 2070, reaching 7.03 million km^2. The Arabian Peninsula shows no climatic suitability, lacking the critical dry-season precipitation (20–80 mm) required by the species. Our findings indicate climate change will significantly expand *G. fuscipes* range, necessitating adaptive, landscape-level vector control strategies. The model definitively excludes Saudi Arabia from the species' potential range, resolving the three-decade controversy.

Supplementary Information The online version contains supplementary material available at https://doi.org/10.1007/s10661-026-15355-5.

M. S. A. El-Hawagry · M. M. Soliman (✉)
Entomology Department, Faculty of Science, Cairo University, Giza, Egypt
e-mail: msoliman@cu.edu.eg

M. S. A. El-Hawagry
e-mail: elhawagry@cu.edu.eg

R. Al-Akeel
Department of Zoology, Faculty of Science, King Saud University, 11451 Riyadh, Saudi Arabia
e-mail: ralogial@ksu.edu.sa

A. Almadiy
Department of Biology, College of Science and Arts, Najran University, 1988 Najran, Saudi Arabia
e-mail: aaalmady@nu.edu.sa

H. M. Al Dhafer
Department of Plant Protection, College of Food and Agricultural Sciences, Chair of Date Palm Research, King Saud University, 11451 Riyadh, Saudi Arabia
e-mail: hdhafer@ksu.edu.sa

Published online: 05 May 2026

Keywords Tsetse fly · African trypanosomiasis · Sleeping sickness · Species distribution modeling · MaxEnt · Climate change

Introduction

Tsetse flies (*Glossina* spp.) are the main vectors of trypanosomes, the protozoan parasites that cause African trypanosomiasis in both humans and livestock (Büscher et al., 2017). The disease is known as sleeping sickness or human African trypanosomiasis (HAT) in humans and as African animal trypanosomiasis (AAT) or nagana in animals (Kennedy, 2013). The most important tsetse fly vectors of trypanosomiasis are *Glossina fuscipes*, *Glossina morsitans*, *Glossina palpalis*, *Glossina pallidipes*, and *Glossina tachinoides*. Of these, *G. fuscipes* is considered the most significant vector for HAT, responsible for an estimated 90% of all reported cases (Büscher et al., 2017).

Understanding the current and future distribution of *G. fuscipes* is critical for multiple reasons. First, as the primary vector responsible for the vast majority of sleeping sickness cases, accurate distribution modeling is essential for public health surveillance, disease risk assessment, and strategic planning of vector control programs. Second, climate change is altering habitats across Africa, potentially expanding or contracting the suitable range for disease vectors, making predictive modeling crucial for proactive intervention strategies. Third, a persistent biogeographical controversy requires resolution: a 1990 report claiming the presence of tsetse flies in Saudi Arabia has created a three-decade-old puzzle with direct implications for disease risk assessment in the Arabian Peninsula.

Elsen et al. (1990) reported two tsetse fly species, *Glossina fuscipes fuscipes* (Newstead, 1910) and *Glossina morsitans submorsitans* (Newstead, 1910), near Gizan (=Gazan, Jizan or Jazan) region in the southwestern part of Saudi Arabia. This was the first and only time these species had been reported outside Africa. Elsen et al. (1990) acknowledged this seemed an odd discovery and attempted to explain the presence of these flies in Saudi Arabia by noting that the southwestern part of the Arabian Peninsula contains comparatively green areas with small permanent watercourses surrounded by bushes and shrubs, which are similar to the habitat of southern Ethiopia and Sudan where these species are found. However, Elsen et al. (1990) questioned the mechanism by which these species arrived at this location and proposed two hypotheses. First, they suggested that the southwest of the Arabian Peninsula may represent a remnant biotope of a much larger distribution area from ancient times, given that the Arabian Peninsula and Africa were once geologically connected millions of years ago, thus potentially justifying the presence of these Afrotropical species (Elsen et al., 1990). Alternatively, Elsen et al. (1990) proposed that the tsetse fly populations in Saudi Arabia may have been accidentally imported with livestock from East Africa, though this hypothesis remains speculative and unsubstantiated.

The study of Elsen et al. (1990) was the only study that reported tsetse flies from Saudi Arabia, and many subsequent studies on the fly fauna of Saudi Arabia using all known collecting techniques could not report any tsetse flies from this region (e.g., El-Hawagry et al., 2013, 2015, 2016, 2017, 2018, 2019). In addition, the authors of the present study have been involved in various projects studying the fly fauna of Saudi Arabia for 15 consecutive years, starting in 2010. One of their objectives was to determine the presence of any tsetse fly species in the region. Despite employing all known collection techniques, they could not collect or observe any tsetse flies.

The known distribution of *G. fuscipes* is centered in central and eastern Africa. It has been verified in 12 Afrotropical countries, including Cameroon, Chad, Central African Republic, South Sudan, Sudan, Ethiopia, Gabon, Congo, Democratic Republic of the Congo, Uganda, Kenya, and the United Republic of Tanzania, though its presence in Rwanda, Burundi, and Zambia remains ambiguous (FAO, 2022). For comparison, the savannah species *G. morsitans* has a much broader distribution, spanning from Senegal in the northwest to Ethiopia in the northeast, and from Angola in the southwest to Mozambique in the southeast (Cecchi et al., 2024; FAO, 1982).

Given the medical importance of *G. fuscipes* as the principal vector of sleeping sickness, the lack of comprehensive distribution projections under climate change scenarios, and the unresolved question of its potential presence in the Arabian Peninsula, species distribution modeling (SDM) using modern approaches such as the maximum entropy model

(MaxEnt) offers a powerful tool to address these knowledge gaps.

MaxEnt has proven particularly effective for predicting tsetse fly distributions under various climate scenarios. Zhou et al. (2021) successfully applied MaxEnt to assess the possible distribution of *G. morsitans*, another medically important tsetse species that was also reported in the controversial 1990 Saudi Arabia record alongside *G. fuscipes* (Elsen et al., 1990). Their modeling approach is directly relevant to our study because both *G. morsitans* and *G. fuscipes* are among the principal vectors of African trypanosomiasis, both were implicated in the same biogeographical anomaly, and both require similar climatic niche assessments to resolve questions about their potential occurrence outside Africa. Zhou et al. (2021) found that the predicted potentially suitable area for *G. morsitans* under historical climate conditions includes a large part of Africa near and below the equator, North and South America, and Oceania, as well as a few small equatorial areas of southern Asia (such as the west of India, Thailand, Cambodia, Myanmar, and Laos). Critically, their model did not predict suitable habitat in Saudi Arabia or any other countries in the Arabian Peninsula, suggesting that similar analytical approaches may help resolve the *G. fuscipes* controversy.

Therefore, the present study aims to (1) model the current potential distribution of *G. fuscipes* across the Afrotropical Region based on verified occurrence records and key environmental variables; (2) project future distributional shifts under multiple climate change scenarios (2050 and 2070) to inform proactive vector management strategies; and (3) definitively assess the climatic suitability of Saudi Arabia and the Arabian Peninsula, testing whether the results for *G. fuscipes* parallel those found for *G. morsitans* and thereby resolving the three-decade-old biogeographical controversy.

Materials and methods

Study area

This study was carried out in the Afrotropical Region, adopting the regional boundaries defined by Kirk-Spriggs and Sinclair (2017). According to this concept, the Afrotropical Region includes the area south of the northern borders of Mauritania, Mali, Niger, Chad, and Sudan, as well as Yemen, Oman, and the UAE. Furthermore, we adopted a broader definition of the region, as proposed by Sclater (1858), Wallace (1876), El-Hawagry and Al Dhafer (2019), and El-Hawagry et al. (2022), which extends the Afrotropical Region northwards into the Arabian Peninsula, up to the Tropic of Cancer. This extended concept encompasses the southwestern provinces of Saudi Arabia, including Al-Baha, Asir, Jazan, and Najran. The study area and the spatial distribution of occurrence records used in this analysis are shown in Fig. 1. The study area fully encompasses the known distribution range of *Glossina fuscipes* in East and Central Africa and extends into regions where the species has not been recorded, enabling both assessment of potential range expansion under climate change and independent evaluation of Arabian Peninsula suitability.

Occurrence data and spatial filtering

Occurrence data for *G. fuscipes* were compiled from published literature and the Global Biodiversity Information Facility (GBIF, 2025), including peer-reviewed articles, technical reports, regional surveys, and biodiversity databases. A complete list of data sources is provided in S1 File. After removing records lacking geographic coordinates, duplicates, and spatially erroneous entries, we retained 238 verified occurrence records (26 from GBIF, 212 from literature). All coordinates were verified for spatial accuracy using Google Maps (Google, 2025).

To objectively assess whether Saudi Arabia falls within the climatically suitable range for *G. fuscipes*, we excluded the single record reported by Elsen et al. (1990) from southwestern Saudi Arabia from the model calibration dataset. This exclusion was necessary to avoid circular reasoning including this geographically isolated record would bias the model to predict suitability in that region, thereby preventing an independent evaluation of whether the Arabian Peninsula possesses environmental conditions consistent with the species' verified ecological requirements in Africa.

To reduce spatial autocorrelation and sampling bias, we performed spatial thinning using the spThin package (Aiello-Lammens et al., 2015) in R version 4.4.1. This algorithm iteratively removes spatially clustered occurrence points while

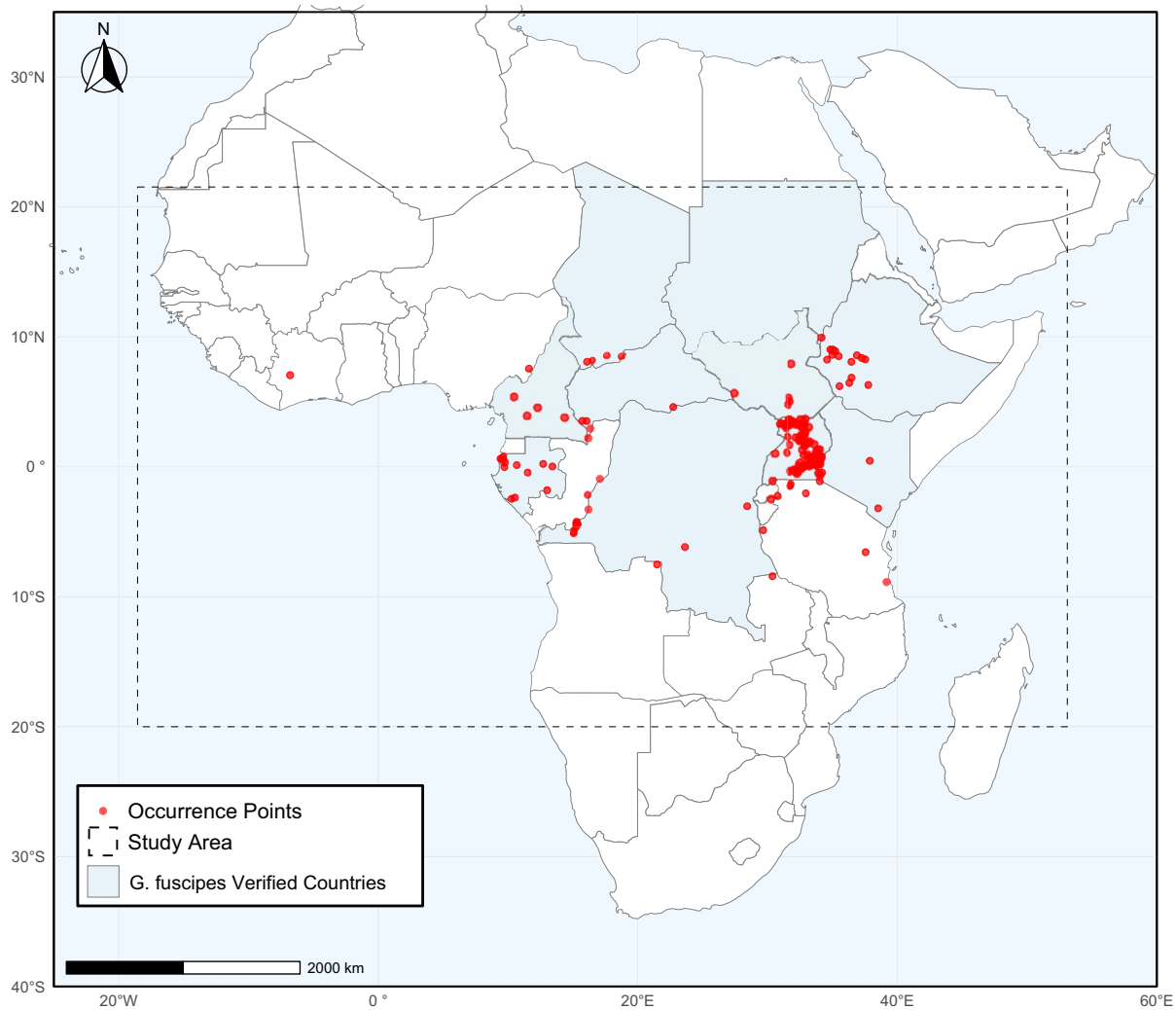

Fig. 1 Study area and occurrence records of *Glossina fuscipes* used in species distribution modeling. The map shows the Afrotropical Region (study area boundary shown by dashed line), including the extended definition that encompasses southwestern Saudi Arabia. Red dots indicate the 158 spatially filtered records used for model calibration after removing redundant points within 5-arcminute grid cells. The blue shading represents the *G. fuscipes*-verified countries

maximizing the number of retained records that maintain a minimum inter-point distance. Given the continental extent of our study area and the need to minimize spatial autocorrelation, we applied a thinning distance of 10 km. This threshold represents a conservative compromise between ecological realism—acknowledging that *G. fuscipes* is a low-dispersal insect—and the practical necessity of ensuring spatial independence at a broad geographic scale. We note that while thinning at this resolution may omit some fine-gradient environmental variation, sensitivity tests using finer distances (e.g., 2 km and 5 km) produced qualitatively similar projections of habitat suitability and range shifts, supporting the robustness of our continental-scale conclusions. The algorithm was run for 100 iterations with random point selection (set.seed = 123 for reproducibility). This procedure yields a final dataset of 158 spatially independent occurrence points (Fig. 1), reducing over-representation of intensively surveyed locations such as northern Uganda and western Ethiopia where disease surveillance programs have concentrated sampling effort.

Table 1 Percent contributions and permutation importance of the environmental variables in the MaxEnt models for *Glossina fuscipes* based on ten replicates

Variables	Description	% contribution	Permutation importance
Bio 14	Precipitation of driest month	41.7	6.7
Alt	Altitude in meters	15.7	15.5
Bio 12	Annual precipitation	14.2	33.4
Bio 9	Mean temperature of driest quarter	10	18.3
Bio 19	Precipitation of coldest quarter	8.4	3.8
Bio 4	Temperature seasonality (coefficient of variation)	5	3.3
Bio 15	Precipitation seasonality (coefficient of variation)	4.9	19

Sampling bias correction

Geographic sampling bias poses a significant challenge when occurrence records reflect spatial patterns of survey effort rather than random sampling. For *G. fuscipes*, sampling has been concentrated in areas with active sleeping sickness control programs and accessible research sites. To address this bias beyond spatial thinning, we implemented bias-corrected background point selection using a bias file approach (Phillips et al., 2009).

The bias file was generated using SDMtoolbox 2.0 (Brown, 2014; Brown et al., 2017) in ArcGIS 10.7. The "Create Bias File" tool constructs a Gaussian kernel density surface based on the spatial distribution of occurrence records, estimating relative sampling effort across the study region. This bias surface was then used in MaxEnt to weight background point selection: 10,000 background points were sampled with probability proportional to the bias surface values, ensuring that presences are compared against background conditions from similarly sampled areas. This approach minimizes the confounding effect of heterogeneous sampling intensity on environmental comparisons (Phillips et al., 2009).

Environmental variables

This investigation employed two principal categories of environmental predictor variables: bioclimatic variables ($n = 19$) and topographic parameters (elevation) (S2 File). To address temporal alignment between occurrence records (1982–2023) and environmental predictors, we obtained monthly climate data from TerraClimate (Abatzoglou et al., 2018) via Google Earth Engine (Gorelick et al., 2017). For the period 1982–2023, we downloaded monthly maximum temperature, monthly minimum temperature, and monthly total precipitation data as GeoTIFF files at approximately 4 km spatial resolution, pre-clipped to the Afrotropical Region. Long-term climatological means were calculated across this 42-year period for each month, and the 19 bioclimatic variables (Bio 1–Bio 19) were subsequently derived from these monthly averages using the terra package in R version 4.4.1. This approach ensures that environmental predictors represent the actual climatic conditions experienced by *G. fuscipes* populations during the observation period (1982–2023), thereby maintaining pseudo-equilibrium assumptions fundamental to correlative species distribution modeling while capturing post-2000 climate warming. The resulting bioclimatic layers were resampled to 30 arc-second spatial resolution (approximately 1 km^2) to match the resolution required for MaxEnt modeling and future climate projections. Elevation data were obtained from WorldClim database version 2.1 (Fick & Hijmans, 2017; https://worldclim.org/data/worldclim21.html) at 30 arc-second spatial resolution.

Variable selection was conducted through a rigorous, noncircular protocol to minimize multicollinearity while maintaining ecological relevance. Unlike preliminary screening methods that rely on model output, we performed a formal variance inflation factor (VIF) analysis on the initial set of 20 variables prior to model fitting using the usdm package in R. We employed a stepwise removal procedure with a strict VIF threshold of 5 (S3 File). This statistically robust approach identified and excluded highly collinear variables that could destabilize model coefficients or inflate variable importance metrics. The final selection comprised seven variables (Table 1) that capture the fundamental environmental axes governing the distribution of the riverine tsetse

species, *G. fuscipes*. These include variables representing water availability and stability, which are critical for a species dependent on high humidity and permanent watercourses: Bio 14 (precipitation of driest month), Bio 12 (annual precipitation), Bio 19 (precipitation of coldest quarter), and Bio 15 (precipitation seasonality). Thermal stability was represented by Bio 4 (temperature seasonality) and Bio 9 (mean temperature of driest quarter), while altitude was retained to account for topographic context.

All environmental layers were standardized to the study area boundaries and converted to ASCII format using ArcGIS 10.7 (ESRI, 2018). MaxEnt internally normalizes variables during training; therefore, no additional manual standardization was applied (Elith et al., 2011). Variable importance was evaluated using two complementary metrics: percent contribution, representing the relative contribution during training, and permutation importance, which measures the decrease in AUC when values are randomly permuted (Phillips et al., 2006). These metrics measure different aspects of variable importance and were considered in tandem when interpreting environmental drivers (Elith et al., 2011).

Future climate projections

Projected future distribution patterns were modeled using climate data derived from five General circulation models (GCMs): GFDL-ESM4, IPSL-CM6A-LR, MPI-ESM1-2-HR, MRI-ESM2-0, and UKESM1-0-LL. High-resolution datasets (30 arc-seconds) for the mid-century (2050; 2040–2060) and late-century (2070; 2060–2080) periods were sourced from the WorldClim database (Fick & Hijmans, 2017). These projections were based on two contrasting shared socioeconomic pathways (SSPs): SSP1-2.6, representing a low-emission scenario, and SSP5-8.5, representing a high-emission scenario ((O'Neill et al., 2016; Riahi et al., 2017). To account for structural uncertainty among climate models and avoid dependence on any single projection, we adopted a multimodel climate ensemble approach (Knutti et al., 2010). For each SSP and time period, the calibrated species distribution model was projected independently onto the climatic layers of each GCM, producing five future suitability surfaces. A final consensus projection was created by computing the pixel-wise arithmetic mean of these continuous suitability scores. The selected GCMs form part of the core ensemble recommended by the Inter-Sectoral Impact Model Intercomparison Project (ISIMIP3b) (Lange et al., 2020), ensuring representation of the key climate sensitivities within CMIP6 (Eyring et al., 2016). Complete model specifications are provided in S4 File.

MaxEnt model implementation and parameterization

Species distribution modeling was performed using MaxEnt version 3.4.4 (Phillips et al., 2024), selected for its robust performance with presence-only data and relatively limited sample sizes (Elith et al., 2006; Phillips et al., 2006), particularly for climate change projections (Yan et al., 2020). MaxEnt contrasts species presence records with background points to estimate habitat suitability, producing continuous habitat suitability maps with values from 0 (unsuitable) to 1 (optimal) (Gebrewahid et al., 2020; Khanum et al., 2013). Background points (10,000) were sampled using the bias file described above, with selection probability proportional to estimated sampling effort. This bias-corrected background sampling was implemented using the "bias file" option in MaxEnt.

Model validation used bootstrap replication with ten replicates. In each replicate, 75% of occurrence records were randomly selected for training and 25% withheld for testing. To minimize overfitting, we systematically tuned MaxEnt's complexity through the regularization multiplier (RM). The default "auto features" setting was used, allowing MaxEnt to automatically select appropriate feature types based on sample size. RM values of 0.5, 1.0, 1.5, and 2.0 were tested to identify optimal balance between complexity and predictive performance (Morales et al., 2017). Final model selection was guided by AICc, which penalizes complexity to prevent overfitting (Warren & Seifert, 2011). The model with RM = 1.0 yielded the lowest AICc and was adopted for final modeling.

Model performance was evaluated using area under the receiver operating characteristic curve (AUC) and true skill statistic (TSS). AUC measures discrimination ability across all thresholds (values > 0.7 acceptable, > 0.8 good, and > 0.9 excellent; Swets, 1988). TSS evaluates classification accuracy at a specific threshold (values > 0.5 indicate good performance, > 0.6 very good; Allouche et al., 2006). These independent metrics assess different aspects

of model quality following best practices (Liu et al., 2011; Sofaer et al., 2019).

Threshold selection and binary classification

To assess potential shifts in species distributions under future climate scenarios, continuous suitability outputs from MaxEnt were transformed into binary presence–absence maps using threshold-based classification. We employed the "10th percentile training presence" threshold, which classifies as suitable all areas with predicted suitability values at or above the value corresponding to the lowest 10% of training presence locations. This threshold was selected primarily because for disease vector distribution modeling, underestimating potentially suitable habitat (false negatives) poses a greater public health risk than overestimation (Barve et al., 2011; Peterson et al., 2008). The 10th percentile threshold maintains high sensitivity, thereby prioritizing the identification of regions at potential risk. Furthermore, this approach accommodates known spatial inaccuracies in georeferenced occurrence records and includes marginal habitats that may become more suitable under future climate scenarios (Pearson et al., 2007). Its use also facilitates comparability with previous tsetse fly distribution studies (e.g., Zhou et al., 2021). Binary maps compared current conditions against future scenarios (SSP1-2.6 and SSP5-8.5 for 2050 and 2070) to quantify four change categories: stable presence (suitable under both current and future), expansion (newly suitable), contraction (loss of suitability), and stable absence (unsuitable under both).

Multimodel climate projections and synthesis

A total of 20 future habitat suitability projections were produced by projecting the calibrated MaxEnt model onto five GCM climate scenarios, across two SSP scenarios, for two time periods. Current potential distributions were estimated by averaging continuous habitat suitability outputs from ten bootstrap replicates. For future projections, we calculated mean continuous suitability values across the five GCM projections within each SSP–time period combination (e.g., averaging across all five GCMs for SSP1-2.6 in 2050). This multimodel climate averaging approach accounts for uncertainty in future climate conditions while maintaining the same ecological model structure (Araújo & New, 2007; McSweeney et al., 2015).

Results

The species distribution model for *Glossina fuscipes* exhibited high predictive performance, achieving a mean training area under the curve (AUC) value of 0.940 ± 0.006 (SD), a test AUC of 0.931 ± 0.021, and a mean true skill statistic (TSS) of 0.681 ± 0.072 (SD) across ten bootstrap replicates. These metrics substantially exceed the recognized performance thresholds for reliable models ($AUC > 0.7$ and $TSS > 0.5$), indicating a strong ability to discriminate between suitable and unsuitable habitats (Fig. 2 and S5 File).

Variable importance analysis reveals that precipitation-related factors and topography are the primary determinants of *G. fuscipes* distribution (Fig. 3 and Table 1). According to percent contribution values, precipitation of the driest period (Bio 14) was the most significant driver, accounting for 41.7% of the model's explanatory power. This was followed by altitude (15.7%), annual precipitation (Bio 12, 14.2%), and the mean temperature of the driest quarter (Bio 9, 10.0%). Together, these four variables contributed over 81% to the model. Permutation importance values, which provide a more robust assessment by measuring the model's dependence on specific variables (Phillips et al., 2006), show that annual precipitation (Bio 12) had the highest impact at 33.4%. Notably, precipitation seasonality (Bio 15) and mean temperature of the driest quarter (Bio 9) show significantly higher permutation importance (19.0% and 18.3%, respectively) than their initial percent contributions, suggesting these variables contain critical predictive information essential for model stability across different geographic regions (Table 1). The jackknife test further corroborates these findings, showing that Bio 15 and Bio 14 provide the highest regularized training gain when used in isolation, indicating they contain the most useful information for predicting the species' distribution (Fig. 3).

The MaxEnt model response curves for *G. fuscipes* reveal distinct climatic preferences that align with specific, and often limited, environmental conditions available across the Afrotropical Region (Fig. 4). For precipitation of driest month (Bio 14), the species

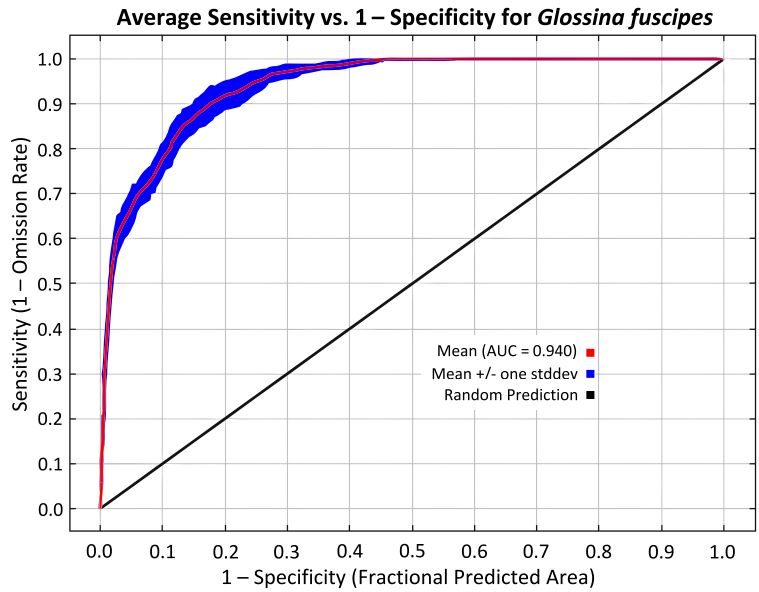

Fig. 2 Reliability test of the distribution model created for *Glossina fuscipes* (values represent averages calculated across ten replicate runs)

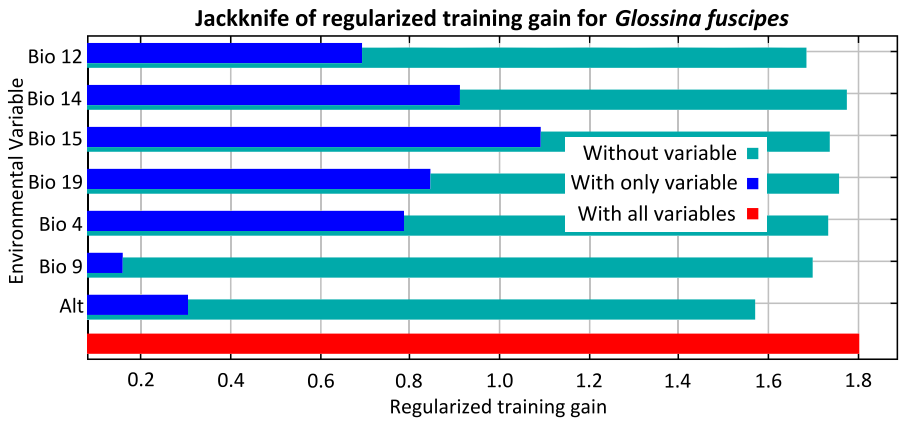

Fig. 3 Jackknife test results for *Glossina fuscipes*, showing the relative importance of each environmental variable in predicting the fly distribution

exhibited optimal habitat suitability at values between 20 and 80 mm, indicating a requirement for consistent moisture availability even during the driest months—a pattern characteristic of humid riverine corridors and perennial water systems. For annual precipitation (Bio 12), the model showed a clear requirement for high rainfall, with a sharp increase in suitability above 800 mm and peak suitability between 1200 and 2000 mm. This range of precipitation is largely restricted to Central Africa and parts of the East African highlands, underscoring the species' dependence on these humid refugia. The altitudinal response (Alt) shows a distinct unimodal pattern. Suitability remains low in coastal and low-lying areas (0–500 m) but increases rapidly to a maximum peak between 1100 and 1300 m. While the species continues to find suitable habitat at higher elevations, the probability of presence gradually tapers off above 2000 m, confirming a preference for mid-elevation highland habitats. Mean temperature of driest quarter (Bio 9) showed optimal suitability within a relatively narrow range (20–30 °C), reflecting the species' requirement for thermally moderate conditions that avoid both extreme heat and cold stress. Collectively, these response patterns indicate that *G. fuscipes* is adapted to humid, thermally stable tropical environments with reliable year-round moisture availability and consistent precipitation regimes.

The species distribution modeling reveals that *G. fuscipes* currently occupies approximately 3,643,572

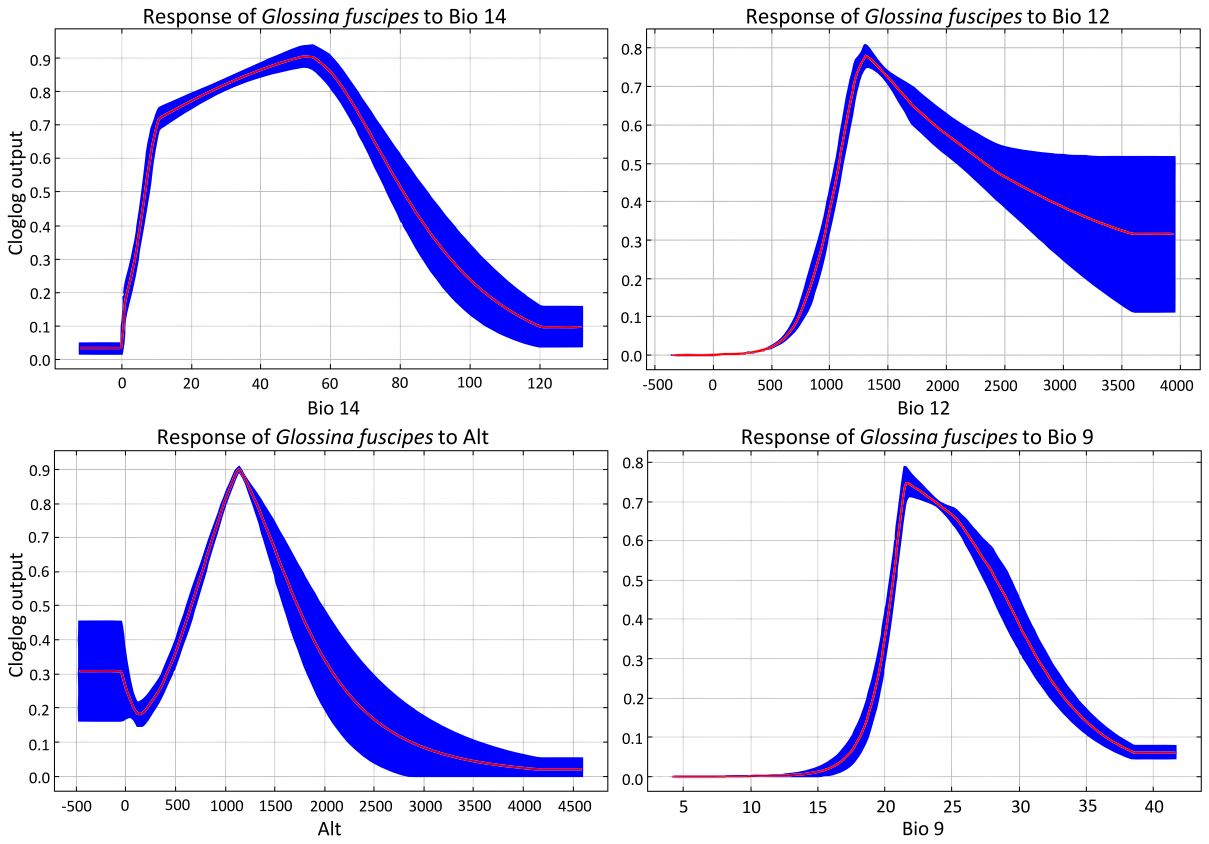

Fig. 4 Response curves of *Glossina fuscipes* to bioclimatic predictors, showing average values across ten replicate runs

km^2 of climatically suitable habitat across the Afrotropical Region, representing 16.7% of the total continental area (Fig. 5). The current distribution shows concentrated areas of high suitability primarily in the East African region, particularly across Uganda, Kenya, Western Ethiopia, and parts of Tanzania. Secondary zones of moderate-to-high suitability extend through the Central African Republic, Democratic Republic of Congo, Cameroon, Rwanda, Burundi, and parts of South Sudan. The western regions of Africa, including most of West Africa, show predominantly low suitability, while Southern Africa exhibits similarly low environmental favorability for the species.

Climate projections indicate substantial changes in the potential distribution of *G. fuscipes* across Africa under both moderate (SSP1-2.6) and high-emission (SSP5-8.5) scenarios for 2050 and 2070 (Figs. 6 and 7; S6 File). The modeling results reveal consistent patterns of range expansion with varying magnitudes depending on the emission pathway and time horizon examined.

Under the moderate emission scenario (SSP1-2.6), the suitable habitat for *G. fuscipes* is projected to expand significantly by 2050, reaching 4,777,649 km^2 and covering 21.95% of Africa. This represents a net increase of 1,134,077 km^2 compared to current conditions. The expansion is characterized by a 38.09% increase in suitable area, while only 3.48% of currently suitable habitat is projected to become unsuitable, indicating a predominantly favorable shift in climatic conditions for the species. The high emission scenario (SSP5-8.5) projects even more substantial habitat expansion by 2050, with suitable areas increasing to 5,787,942 km^2, covering 26.59% of Africa. This scenario shows a remarkable 62.25% expansion of suitable habitat area, while habitat contraction affects only 1.70% of currently suitable regions. The net gain under this scenario amounts to approximately 2,144,370 km^2.

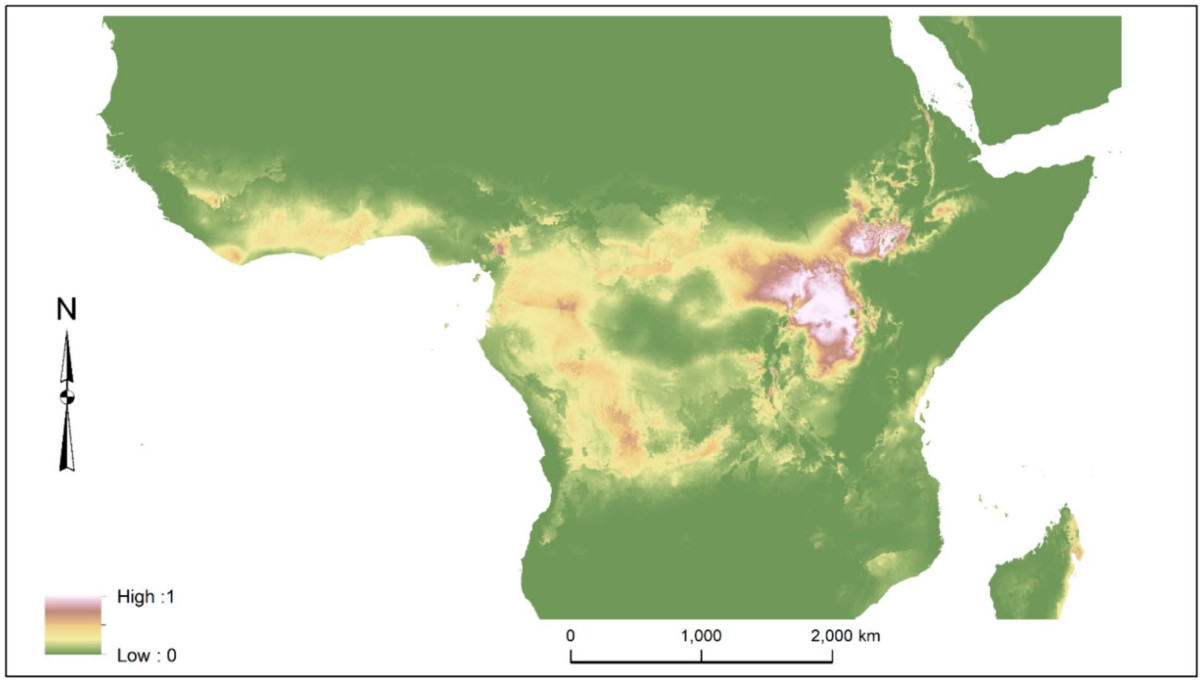

Fig. 5 Potential environmental suitability map for *Glossina fuscipes* in the Afrotropical Region, based on occurrence records, highlighting areas environmentally favorable to the species

By 2070, the moderate-emission scenario projects continued expansion of suitable habitat to 5,155,280 km^2, representing 23.68% of Africa. The area expansion reaches 46.97%, while habitat contraction decreases to 2.74% of current suitable areas, suggesting increasingly favorable conditions for *G. fuscipes* establishment across broader geographic ranges. The high-emission scenario for 2070 presents the most dramatic changes, with suitable habitat expanding to 7,027,244 km^2, covering 32.29% of the African continent. This scenario projects an unprecedented 95.03% expansion of suitable areas while experiencing only 1.08% habitat contraction. The projected suitable area represents nearly double the current distribution, indicating profound shifts in the species' potential range.

The future distribution maps reveal distinct spatial patterns in habitat suitability changes. Under both scenarios and time periods, the core areas of high suitability in East-Central Africa maintain their optimal conditions while expanding outward. Notable expansions are projected in West Africa, where countries such as Nigeria, Cameroon, and coastal West African nations show increased suitability values compared to current conditions. The Sahel region displays particular sensitivity to climate change, with moderate emission scenarios showing gradual northward expansion of suitable habitat, while high emission scenarios project more dramatic shifts.

Southern Africa demonstrates variable responses between scenarios, with the high-emission pathway (SSP5-8.5) showing greater expansion into previously unsuitable areas compared to the moderate scenario. The Democratic Republic of the Congo shows consistent expansion potential under all scenarios, suggesting this region may become increasingly important for *G. fuscipes* populations.

Discussion

This study projected the current and future potential distribution of *Glossina fuscipes*, a primary vector of human African trypanosomiasis, using climatic variables and topographic data. Our results indicate that among the environmental variables examined, the species' distribution is strongly associated with precipitation of the driest period (Bio 14), altitude, annual precipitation (Bio 12), and mean temperature

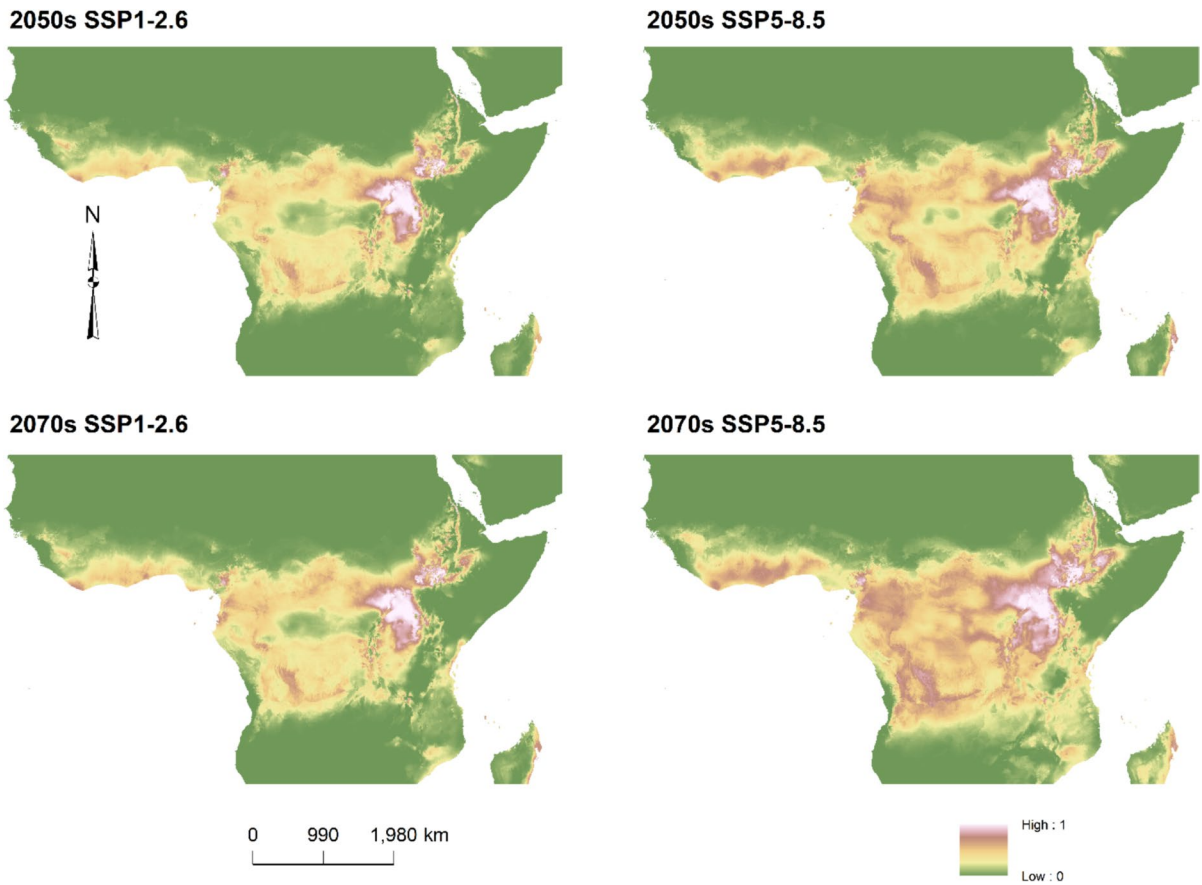

Fig. 6 Predicted future distribution of *Glossina fuscipes* in the Afrotropical Region under two climate change scenarios (SSP1-2.6 and SSP5-8.5) for 2050 (2041–2060) and 2070 (2061–2080). Maps show the spatial extent and intensity of environmental suitability based on projected climatic conditions

of the driest quarter (Bio 9). The current suitable habitat, estimated at approximately 3.64 million km^2, is concentrated in East and Central Africa. Critically, our future projections under both low- (SSP1-2.6) and high-emission (SSP5-8.5) scenarios forecast a substantial net expansion of suitable habitat by 2050 and 2070, suggesting an escalating risk of trypanosomiasis transmission across the African continent.

Our findings align with and, in some respects, refine the existing body of literature that has explored the environmental drivers of tsetse fly distribution at more localized scales (Duguma et al., 2015; Longbottom et al., 2024; Mugenyi et al., 2021; Saarman et al., 2018). The preference of *G. fuscipes* for humid, thermally stable environments with consistent, high rainfall is a recurrent theme that emerges when comparing our results to previous research conducted across multiple regions of Africa (Akinseye et al., 2024; Kargbo et al., 2025; Messina et al., 2012; Moore et al., 2012; Zhou et al., 2021). Our model's identification of precipitation of the driest period (Bio 14) as the single most important predictor (41.7% contribution) represents a significant refinement of previous understanding. This variable's dominance emphasizes that *G. fuscipes* survival depends not merely on high total annual rainfall, but critically on the maintenance of minimum moisture thresholds during the driest months. This finding strongly corroborates the well-documented association of *G. fuscipes* with perennial riverine and lacustrine habitats that provide reliable year-round water availability (Longbottom et al., 2024; Mugenyi et al., 2021).

The requirement for dry-season precipitation (20–80 mm) and high annual rainfall (> 800 mm,

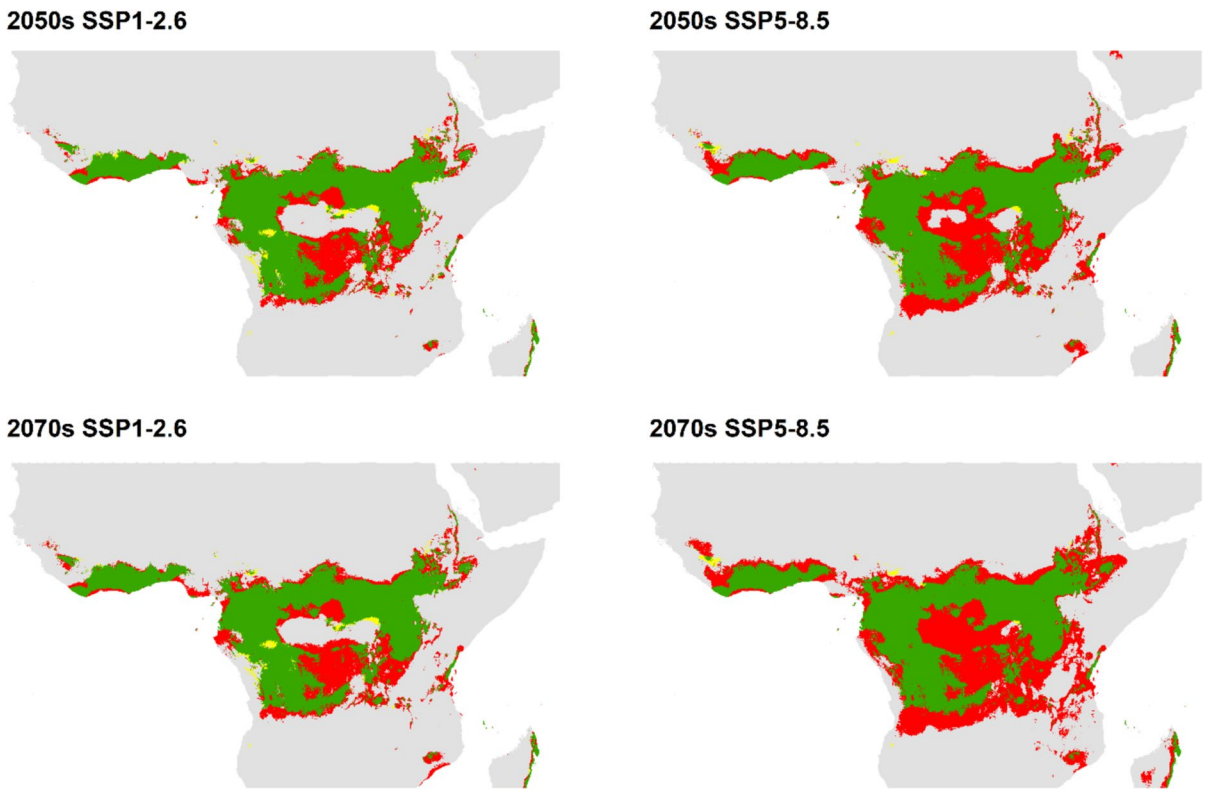

Fig. 7 Summary of predicted *Glossina fuscipes* distribution in the Afrotropical Region under current and future conditions (2050, 2070) across the SSP1-2.6 and SSP5-8.5 scenarios. Green areas indicate consistent presence (current and future); red areas show potential habitat expansion; and yellow represents possible contraction. This binary map simplifies the continuous suitability values from Figs. 5 and 6

optimally 1200–2000 mm) directly supports the presence of permanent water bodies and the dense riparian vegetation that tsetse flies depend on for survival—key findings from studies showing tsetse abundance is positively correlated with rainfall and proximity to rivers (Longbottom et al., 2024; Mugenyi et al., 2021). The connection between water, humidity, and vegetation is critical for tsetse fly survival and reproduction. Saarman et al. (2018) found that *G. f. fuscipes* prefers habitats with high humidity, which are typically found near water sources that sustain dense vegetation growth. Similarly, the positive correlation between tsetse presence and Normalized Difference Vegetation Index (NDVI) reported by multiple studies (Longbottom et al., 2024; Messina et al., 2012; Mugenyi et al., 2021) can be seen as a direct consequence of the climatic conditions our model identified. High and stable precipitation, particularly during dry periods, serves as a prerequisite for the high NDVI values and net photosynthesis (PSN) that characterize suitable tsetse habitats (Saarman et al., 2018).

However, it is important to acknowledge that our SDM approach identifies climatically suitable areas based on correlations between species occurrences and environmental variables, rather than establishing direct causation. Our model represents potential climatic suitability and does not account for other critical factors that determine realized distributions, such as land use change, urbanization, agricultural expansion, habitat fragmentation, or host availability. As demonstrated by De Deken et al. (2005) in the DRC, agricultural-driven habitat modification can substantially reduce tsetse populations even within climatically favorable zones. Therefore, our bioclimatic predictors should be considered foundational drivers that identify the broad climatic envelope within which the species could potentially

persist, rather than definitive predictions of actual presence.

The high permutation importance of annual precipitation (Bio 12, 33.4%) despite its lower percent contribution (14.2%) reveals an important distinction in how this variable functions within the model. Permutation importance measures how much model accuracy decreases when a variable's values are randomly shuffled, thus reflecting the variable's unique contribution to predictive power that cannot be compensated for by other variables (Phillips et al., 2006). The substantial difference between Bio 12's permutation importance and percent contribution suggests it captures precipitation information at different temporal scales or geographic contexts than Bio 14, providing complementary rather than redundant climatic information. This dual importance of both total annual precipitation and dry-season precipitation underscores the species' requirement for both high overall moisture availability and temporal consistency—characteristics that define stable riverine ecosystems.

The significance of mean temperature of the driest quarter (Bio 9) in our model (10% contribution, 18.3% permutation importance) highlights a previously underappreciated aspect of *G. fuscipes* thermal ecology. While previous studies have emphasized general temperature requirements (Akinseye et al., 2024; Kargbo et al., 2025; Moore et al., 2012), our results reveal that thermal conditions specifically during the driest period are critical. The narrow optimal range (20–30 °C) during dry months suggests that the species is vulnerable to thermal extremes precisely when water-dependent microhabitat buffering is most stressed. This finding resonates with studies on the related *morsitans* group, where thermal stability was found to be a primary predictor of distribution (Muyobela et al., 2023; Zhou et al., 2021) and explains why tsetse flies are often confined to buffered microclimates within forests and dense woodlands (Duguma et al., 2015; Mugenyi et al., 2021).

The altitudinal response of *G. fuscipes* in our model reveals a distinct unimodal pattern with peak suitability at mid-elevations (1100–1300 m), contrasting with some regional studies that documented straightforward inverse relationships between tsetse abundance and altitude (Duguma et al., 2015; Longbottom et al., 2024; Mugenyi et al., 2021). This mid-elevation optimum, derived from continental-scale occurrence data using climate variables, likely reflects zones where orographic precipitation creates reliable moisture availability while temperatures remain within tolerable ranges. Highland areas at these elevations may provide an optimal balance of key climatic factors: they are cool enough to avoid thermal stress but receive high and consistent rainfall, creating ideal conditions that may be less common in hotter, more seasonal lowlands or in excessively cold high-elevation zones. The simpler inverse relationships observed in some regional studies may represent localized gradients within specific geographic contexts, whereas our continental model captures the full complexity of altitudinal responses across diverse African mountain systems.

The species distribution model developed in this study predicts that *G. fuscipes* currently finds approximately 3.64 million km^2 of climatically suitable habitat across the Afrotropical Region. This estimated range provides a species-specific refinement to broader estimates for the entire *Glossina* genus, which have been placed at around 8.7 million km^2 (Bakhoum et al., 2021). The geographic pattern of this suitable habitat, with its pronounced concentration in East and Central Africa, is strongly corroborated by numerous regional and local studies.

The model's identification of Uganda as a primary stronghold for *G. fuscipes* aligns precisely with extensive field research. Studies in northern Uganda have consistently identified large, well-connected areas of suitable habitat and high tsetse abundance, particularly in riverine landscapes (Longbottom et al., 2024; Saarman et al., 2018). Our model's prediction of high suitability across the country is further validated by the work of Mugenyi et al. (2021), who documented high tsetse populations along the shores of Lakes Victoria, Kyoga, and Albert, and within major game reserves. Similarly, the predicted suitability in western Ethiopia is consistent with entomological surveys by Duguma et al. (2015), who confirmed the presence of *G. f. fuscipes* in that region. The model also supports an extension of suitable habitat into the Democratic Republic of the Congo (DRC). However, local studies indicate that even within climatically favorable areas, factors such as agricultural-driven habitat fragmentation can result in reduced population densities, particularly near the edges of a subspecies' range (De Deken et al., 2005). De Deken and colleagues further observed that suitable habitats were primarily

confined to narrow buffer zones along river systems, which may account for the patchy distribution pattern predicted by our model in this region.

The projections from our species distribution model indicate that the climatically suitable habitat for *G. fuscipes* is poised for substantial expansion across the Afrotropical Region by 2050 and 2070, under both low-emission and high-emission scenarios. This finding of a net gain in suitable range—potentially nearly doubling by 2070 under SSP5-8.5 (95% expansion)—has profound implications for the future landscape of human and animal African trypanosomiasis. Our results suggest that rather than contracting, the bioclimatic niche for this key vector will become more widely available, pushing its potential distribution into new territories.

This projected expansion for *G. fuscipes*, a member of the riverine *palpalis* group, presents a compelling contrast to the future outlook for many savannah-dwelling species of the *morsitans* group. For instance, studies on *G. morsitans*, *G. pallidipes*, and *G. swynnertoni* in Tanzania and Zimbabwe have predicted overall habitat shrinkage in traditional low-elevation strongholds due to rising temperatures exceeding thermal tolerance limits (Lord et al., 2018; Nnko et al., 2021). Similarly, a continental model for *G. morsitans* projected an overall decline in suitable habitat under future climate scenarios (Zhou et al., 2021). Our results, however, align with the hypothesis put forth by Courtin et al. (2008), who suggested that resilient riverine species like *G. fuscipes* are better adapted to persist and are expected to continue playing a significant role in transmission, whereas savannah species may face decline. The ability of *G. fuscipes* to thrive in buffered, humid riverine microclimates—particularly its dependence on dry-season moisture availability rather than thermal extremes—may confer greater resilience to broad-scale temperature increases compared to its savannah-dwelling relatives.

The remarkably low contraction rates projected across all scenarios (1.08–3.48%) combined with high expansion rates (38–95%) suggest that climate change will create net-positive conditions for *G. fuscipes* across most of its current range while simultaneously opening new suitable areas. This asymmetric response likely reflects that future climate scenarios project both warming and altered precipitation patterns that, on balance, favor the species' moisture-dependent ecology. Increased temperatures at higher elevations may render previously thermally marginal highland areas suitable, while enhanced precipitation in currently semi-arid regions may create new riverine refugia.

The spatial pattern of the projected expansion in our model is also a critical finding and is consistent with trends observed in other studies, even for different species. A key feature of our projections is the expansion of suitable habitat into higher-elevation areas that are currently marginal or unsuitable. This phenomenon has been explicitly predicted for tsetse in the Kenyan Highlands (Messina et al., 2012) and the high-elevation areas of Zimbabwe (Longbottom et al., 2020; Lord et al., 2018), which were previously considered too cold to support tsetse populations. The consistent prediction of upward altitudinal shifts across different models and regions suggests this is a robust and widespread response of tsetse flies to climate warming. Furthermore, our model's projection of newly suitable areas emerging in West Africa and expanding northward toward the Sahel points to a potential reversal of the historical southward range contraction reported by Courtin et al. (2008), which was linked to past decreases in rainfall. Future climate change, particularly increases in temperature and altered precipitation patterns, may render these regions newly hospitable.

The projected habitat expansion of *G. fuscipes* has significant implications for vector control strategies and disease transmission risk. Saarman et al. (2018) identified approximately 20,000 km^2 more suitable habitat than previously recognized at the eastern margin of *G. f. fuscipes* range in northern Uganda, emphasizing that previously "unsuitable" areas might enable tsetse persistence and reinvasion. Our continental-scale projections suggest this pattern may be replicated across much broader geographic ranges, potentially requiring substantial modifications to current control strategies. The identification of 24 isolated patches in northern Uganda by Saarman et al. (2018) provided targets for localized eradication efforts. However, our projections of substantial habitat expansion—particularly the 95% expansion under SSP5-8.5 by 2070—suggest that the number and connectivity of such patches may increase dramatically under future climate scenarios, potentially making isolation-based control strategies less effective and

requiring more comprehensive, landscape-level management approaches.

The species distribution model presented in this study provides compelling evidence against the presence of climatically suitable habitats for *G. fuscipes* in the Arabian Peninsula. As illustrated in the generated distribution map, the entire territory of Saudi Arabia, including the southwestern Gizan region where the flies were reportedly found (Elsen et al., 1990), is characterized by a habitat suitability index approaching zero. This starkly contrasts with the high suitability predicted for the species' known core ranges in East and Central Africa. This result strongly suggests that the environmental and climatic conditions in Saudi Arabia are fundamentally unsuitable for the long-term survival and establishment of *G. fuscipes* populations, particularly given the species' critical requirement for dry-season precipitation (20–80 mm minimum) that is virtually absent in the Arabian Peninsula's arid climate.

This finding aligns perfectly with the extensive, albeit negative, field evidence gathered over the past three decades. Despite numerous and prolonged entomological surveys, including 15 years of dedicated fieldwork by the authors of this study and multiple published faunistic inventories (e.g., El-Hawagry et al., 2013, 2019), no tsetse flies have been collected or observed since the initial 1990 report. Furthermore, our results for *G. fuscipes* are consistent with the MaxEnt modeling for *G. morsitans* conducted by Zhou et al. (2021), which also predicted no suitable habitat in the Arabian Peninsula. While the precise circumstances of the 1990 collection remain unknown—whether it resulted from a transient, nonviable introduction or a potential misidentification—the overwhelming body of evidence indicates that Saudi Arabia is not, and has not been in recent history, part of the natural distribution range of *G. fuscipes*. This resolves the decades-old question and reaffirms the status of tsetse fly–transmitted trypanosomiasis as a uniquely Sub-Saharan African health issue.

While our model demonstrated strong predictive metrics, with a mean training AUC of 0.940, test AUC of 0.931, and TSS of 0.681, the results must be interpreted within the context of several methodological and ecological constraints. First, although we addressed the temporal mismatch concern by using bioclimatic variables calculated from TerraClimate data (1982–2023), the variable selection process was primarily data-driven rather than defined by a priori ecological hypotheses. However, despite this statistical limitation, the final subset of retained variables—particularly precipitation of the driest period (Bio 14), annual precipitation (Bio 12), and mean temperature of the driest quarter (Bio 9)—aligns remarkably closely with the known physiological constraints of *G. fuscipes*. As a riverine species, *G. fuscipes* relies heavily on stable hydrological regimes and buffered microclimates captured by these variables. The dominance of dry-season moisture (Bio 14) as the primary predictor strongly validates this data-driven approach, as it identifies the most biologically critical limiting factor. Thus, while the selection method was statistical, the resulting model remains ecologically interpretable and consistent with the species' requirement for humid, thermally stable environments with year-round water availability.

Second, methodological choices regarding evaluation and thresholding warrant caution. Although AUC scores were high, the TSS exhibited greater variability across bootstrap replicates (SD = 0.072). This instability suggests that classification accuracy is sensitive to the random partitioning of our spatially thinned dataset and that high AUC values may partly reflect the broad discrimination between the species-specific niche and the vast Afrotropical background. In addition, our use of the 10th percentile training presence threshold—selected to prioritize sensitivity for public health surveillance—may inadvertently amplify sampling bias if low-suitability records are clustered in peripheral regions (Freeman & Moisen, 2008; Liu et al., 2005). Consequently, our binary maps should be viewed as visualizations of potential risk rather than definitive presence-absence predictions; for operational planning, continuous suitability surfaces offer more nuanced guidance (Guillera-Arroita et al., 2015).

Third, there is an inherent scale mismatch between our continental analysis and the microhabitats occupied by *G. fuscipes*. By relying on coarse-resolution climatic predictors (~1 km^2), our model identifies the broad "bioclimatic envelope" but necessarily excludes fine-scale drivers such as proximity to water bodies, vegetation structure, host availability, and human population density, all of which influence local distribution (Mugenyi et al., 2021; Saarman et al., 2018). Furthermore, as a correlative model, this

analysis does not account for anthropogenic factors such as agricultural expansion or urbanization, which can suppress tsetse populations even within climatically suitable zones (De Deken et al., 2005). Finally, our future projections rely on the assumption of niche conservatism, presupposing that the species' environmental tolerances will remain stable over time. This does not account for potential evolutionary adaptation or physiological plasticity. Despite these limitations, we believe this model provides a robust, first-order approximation of the climate-driven distributional potential of *G. fuscipes*. Future research should aim to integrate these broad-scale environmental preferences with mechanistic physiological models and local-scale land-use data to develop hierarchically structured predictive frameworks for adaptive vector control.

Conclusions

This study successfully modeled the current and future potential distribution of the principal sleeping sickness vector, *Glossina fuscipes*, providing critical insights for public health and vector control. Our results reveal that the species' distribution is fundamentally governed by year-round water availability, particularly dry-season precipitation, and thermal stability, with its current suitable habitat of approximately 3.64 million km^2 centered in East and Central Africa. The most significant finding is the projected substantial net expansion of the vector's suitable habitat under future climate change, with potential range increases of 38–95% depending on emission scenarios, nearly doubling by 2070 under high-emission pathways. This expansion into previously unsuitable highland and northern regions portends a serious escalation of trypanosomiasis risk, potentially exposing naive human and animal populations. These findings challenge control strategies based on geographic isolation and underscore the urgent need for proactive, adaptive, and landscape-level management to mitigate future transmission. Furthermore, this research demonstrates that the Arabian Peninsula, including Saudi Arabia, lacks suitable climatic conditions for *G. fuscipes* establishment. This finding, supported by three decades of negative field surveys and the species' critical requirement for dry-season moisture absent in Arabian climates, conclusively resolves the controversy surrounding the 1990 report and reaffirms that tsetse-transmitted trypanosomiasis remains a uniquely Sub-Saharan African health challenge.

Acknowledgements The authors would like to acknowledge the support provided by the Deanship of Scientific Research, Ongoing Research Funding program—Research Chairs, King Saud University, Riyadh, Saudi Arabia.

Author contribution M.S. and M.E-H. designed and conceptualized the work. M.S. performed the formal analysis. M.S., R.A-A., A.A., and M.E-H. interpreted the results. M.S., M.E-H., R.A-A., A.A., and H.A-D. prepared the original draft. M.S., M.E-H., R.A-A., A.A., and H.A-D. edited and reviewed the final manuscript. All authors read and approved the final manuscript.

Funding The present study was funded by the Deanship of Scientific Research, Ongoing Research Funding program—Research Chairs (ORF-RC-2025-3800), King Saud University, Riyadh, Saudi Arabia.

Data availability The authors confirm the data supporting the findings are available within this article.

Declarations

Ethics approval and consent to participate All authors have read, understood, and complied as applicable with the statement on the "Ethical Responsibilities of Authors" as found in the Instructions for Authors.

Competing interests The authors declare no competing interests.

References

Abatzoglou, J. T., Dobrowski, S. Z., Parks, S. A., & Hegewisch, K. C. (2018). TerraClimate, a high-resolution global dataset of monthly climate and climatic water balance from 1958–2015. *Scientific Data*, *5*(1). https://doi.org/10.1038/sdata.2017.191

Aiello-Lammens, M. E., Boria, R. A., Radosavljevic, A., Vilela, B., & Anderson, R. P. (2015). spThin: An R package for spatial thinning of species occurrence records for use in ecological niche models. *Ecography, 38*(5), 541–545. https://doi.org/10.1111/ecog.01132

Akinseye, O., Olaleye, O., Sunday, A. J., Otunla, M. T., Edith, A. K., & Mustapha, A. (2024). Population dynamics of tsetse fly in Ido LGA of Oyo state in response to environmental factors and climate change. *MOJ Ecology & Environmental Sciences*, *9*(3), 104–106. https://doi.org/10.15406/mojes.2024.09.00312

Allouche, O., Tsoar, A., & Kadmon, R. (2006). Assessing the accuracy of species distribution models: Prevalence, kappa and the true skill statistic (TSS). *Journal of Applied*

Ecology, 43(6), 1223–1232. https://doi.org/10.1111/j.1365-2664.2006.01214.x

Araújo, M., & New, M. (2007). Ensemble forecasting of species distributions. *Trends in Ecology & Evolution, 22*(1), 42–47. https://doi.org/10.1016/j.tree.2006.09.010

Bakhoum , M. T., Vreysen, M. J. B., & Bouyer, J. (2021). The use of species distribution modelling and landscape genetics for tsetse control. In J. Hendrichs, R. Pereira, & Vreysen, M. J. B (Eds.), *AreaWide Integrated Pest Management: Development and Field Application* (pp. 857–868). Boca Raton, Florida, USA: CRC Press.

Barve, N., Barve, V., Jiménez-Valverde, A., Lira-Noriega, A., Maher, S. P., Peterson, A. T., et al. (2011). The crucial role of the accessible area in ecological niche modeling and species distribution modeling. *Ecological Modelling, 222*(11), 1810–1819. https://doi.org/10.1016/j.ecolmodel.2011.02.011

Brown, J. L. (2014). SDMtoolbox: A python-based GIS toolkit for landscape genetic, biogeographic and species distribution model analyses. *Methods in Ecology and Evolution, 5*(7), 694–700. https://doi.org/10.1111/2041-210x.12200

Brown, J. L., Bennett, J. R., & French, C. M. (2017). SDMtoolbox 2.0: The next generation Python-based GIS toolkit for landscape genetic, biogeographic and species distribution model analyses. *PeerJ*, *5*, e4095. https://doi.org/10.7717/peerj.4095

Büscher, P. G. C., Jamonneau, V., & Priotto, G. (2017). Human African trypanosomiasis. *Lancet, 390*, 2397–2409.

Cecchi, G., Paone, M., de Gier, J., & Zhao, W. (2024). *The continental atlas of the distribution of tsetse flies in Africa. PAAT Technical and Scientific Series, No. 12.* (p. 224). Rome, Italy: FAO . https://openknowledge.fao.org/handle/20.500.14283/cd2022en. Accessed 2025

Courtin, F., Jamonneau, V., Duvallet, G., Garcia, A., Coulibaly, B., Doumenge, J. P., et al. (2008). Sleeping sickness in West Africa (1906-2006): Changes in spatial repartition and lessons from the past. *Tropical Medicine & International Health, 13*(3), 334–344. https://doi.org/10.1111/j.1365-3156.2008.02007.x

De Deken, R., Sumbu, J., Mpiana, S., Mansinsa, P., Watsenga, F., Lutumba, P., et al. (2005). Trypanosomiasis in Kinshasa: Distribution of the vector, *Glossina fuscipes* quanzensis, and risk of transmission in the peri-urban area. *Medical and Veterinary Entomology, 19*(4), 353–359. https://doi.org/10.1111/j.1365-2915.2005.00580.x

Duguma, R., Tasew, S., Olani, A., Damena, D., Alemu, D., Mulatu, T., et al. (2015). Spatial distribution of Glossina sp. and Trypanosoma sp. in south-western Ethiopia. *Parasites & Vectors*, *8*(1). https://doi.org/10.1186/s13071-015-1041-9

El Hawagry , M. S., & Al Dhafer, H. M. (2019). The family Bombyliidae in the Kingdom of Saudi Arabia (Diptera: Brachycera: Asiloidea). *Zootaxa*, *4590*(1), 59. https://doi.org/10.11646/zootaxa.4590.1.3

El-Hawagry, M. S., Abdel-Dayem, M. S., & Al Dhafer, H. M. (2018). A contribution to the knowledge of fly fauna in the Kingdom of Saudi Arabia: New country records and an account of flies identified from Rawdhats, Riyadh Region, with biogeographical remarks (Insecta: Diptera). *Journal of Natural History, 52*(21–22), 1377–1393. https://doi.org/10.1080/00222933.2018.1456575

El-Hawagry, M. S., Abdel-Dayem, M. S., Elgharbawy, A. A., & Al Dhafer, H. M. (2016). A preliminary account of the fly fauna in Jabal Shada al-A'la Nature Reserve, Saudi Arabia, with new records and biogeographical remarks (Diptera, Insecta). *ZooKeys, 636*, 107–139. https://doi.org/10.3897/zookeys.636.9905

El-Hawagry, M. S., Abdel-Dayem, M. S., El-Sonbati, S. A., & Al Dhafer, H. (2017). A preliminary account of the fly fauna in Garf Raydah Nature Reserve, Kingdom of Saudi Arabia, with new records and biogeographical remarks (Diptera: Insecta). *Journal of Natural History, 51*(25–26), 1499–1530. https://doi.org/10.1080/00222933.2017.1347299

El-Hawagry, M., Al-Khalaf, A. A., Soliman, A. M., Abdel-Dayem, M. S., & Al Dhafer, H. M. (2022). The Nemestrinidae in Egypt and Saudi Arabia (Brachycera: Diptera). *Egyptian Journal of Biological Pest Control, 32*(1), 26. https://doi.org/10.1186/s41938022005257

El-Hawagry, M., Khalil, M., Sharaf, M., Fadl, H., & Aldawood, A. (2013). A preliminary study on the insect fauna of Al-Baha Province, Saudi Arabia, with descriptions of two new species. *ZooKeys, 274*, 1–88. https://doi.org/10.3897/zookeys.274.4529

El-Hawagry, M. S., Sharaf, M. R., Al Dhafer, H. M., Fadl, H. H., & Aldawood, A. S. (2015). Addenda to the insect fauna of Al-Baha Province, Kingdom of Saudi Arabia with zoogeographical notes. *Journal of Natural History, 50*(19–20), 1209–1236. https://doi.org/10.1080/00222933.2015.1103913

El-Hawagry, M. S., Al Dhafer, H. M., & Abdel-Dayem, M. S. (2019). On the fly fauna of the central region of the Kingdom of Saudi Arabia: New country records from Riyadh Region, with a list of associated fly species and zoo geographical remarks (Insecta: Diptera). *Journal of Natural History, 53*(1–2), 17–43. https://doi.org/10.1080/00222933.2019.1568601

Elith, J., H. Graham, C., P. Anderson, R., Dudík, M., Ferrier, S., Guisan, A., et al. (2006). Novel methods improve prediction of species' distributions from occurrence data. *Ecography*, *29*(2), 129–151. https://doi.org/10.1111/j.2006.0906-7590.04596.x

Elith, J., Phillips, S. J., Hastie, T., Dudík, M., Chee, Y. E., & Yates, C. J. (2011). A statistical explanation of MaxEnt for ecologists. *Diversity and Distributions, 17*(1), 43–57. https://doi.org/10.1111/j.1472-4642.2010.00725.x

Elsen, P., Amoudi, M., & Leclercq, M. (1990). First record of *Glossina fuscipes* fuscipes Newstead, 1910 and Glossina morsitans submorsitans Newstead, 1910 in southwestern Saudi Arabia. *Annales de la Societe belge de medecine tropicale*, *70*(4), 281–287. http://europepmc.org/abstract/MED/2291693

ESRI. (2018). *ArcGIS Desktop: Release 10.7*. Redlands, CA: Environmental Systems Research Institute.

Eyring, V., Bony, S., Meehl, G. A., Senior, C. A., Stevens, B., Stouffer, R. J., & Taylor, K. E. (2016). Overview of the Coupled Model Intercomparison Project Phase 6 (CMIP6) experimental design and organization. *Geoscientific Model Development, 9*(5), 1937–1958. https://doi.org/10.5194/gmd-9-1937-2016

FAO. (1982). *Ecology and behaviour of tsetse (J. N. Pollock, Ed.). Training manual for tsetse control personnel*

(Vol. 2). (J. Pollock, Ed.) (p. 101). Food and Agriculture Organization of the United Nations. https://openknowledge.fao.org/server/api/core/bitstreams/de6d9791-0f4e-4fd3-804d-28ddbb701930/content. Accessed 10 July 2025

FAO. (2022). *Programme Against African Trypanosomiasis (PAAT): Tsetse distribution*. Food and Agriculture Organization of the United Nations. [https://www.fao.org/paat/en/]

Fick, S. E., & Hijmans, R. J. (2017). WorldClim 2: new 1-km spatial resolution climate surfaces for global land areas. *International Journal of Climatology, 37*(12), 4302–4315.

Freeman, E. A., & Moisen, G. G. (2008). A comparison of the performance of threshold criteria for binary classification in terms of predicted prevalence and kappa. *Ecological Modelling, 217*(1–2), 48–58. https://doi.org/10.1016/j.ecolmodel.2008.05.015

GBIF.org. (2025). GBIF Occurrence Download. https://www.gbif.org/occurrence/search?taxon_key=5056011. Accessed 1 January 2025

Gebrewahid, Y., Abrehe, S., Meresa, E., Eyasu, G., Abay, K., Gebreab, G., et al. (2020). Current and future predicting potential areas of Oxytenanthera abyssinica (A. Richard) using MaxEnt model under climate change in Northern Ethiopia. *Ecological Processes, 9*(1). https://doi.org/10.1186/s13717-019-0210-8

Google. (2025). Google Maps. Google LLC. https://www.google.com/maps. Accessed 1 April 2025

Gorelick, N., Hancher, M., Dixon, M., Ilyushchenko, S., Thau, D., & Moore, R. (2017). Google Earth Engine: Planetary-scale geospatial analysis for everyone. *Remote Sensing of Environment, 202*, 18–27. https://doi.org/10.1016/j.rse.2017.06.031

Guillera-Arroita, G., Lahoz-Monfort, J. J., Elith, J., Gordon, A., Kujala, H., Lentini, P. E., et al. (2015). Is my species distribution model fit for purpose? Matching data and models to applications. *Global Ecology and Biogeography, 24*(3), 276–292. https://doi.org/10.1111/geb.12268

Kargbo, A., Dafka, S., Osman, A. M., Koua, H. K., Rafael, F., & Rocklöv, J. (2025). Impact of climate change and variability on the occurrence and distribution of Trypanosoma vectors in The Gambia. *Parasitology Research, 124*(3). https://doi.org/10.1007/s00436-025-08475-3

Kennedy, P. G. (2013). Clinical features, diagnosis, and treatment of human African trypanosomiasis (sleeping sickness). *The Lancet Neurology, 12*(2), 186–194. https://doi.org/10.1016/s1474-4422(12)70296-x

Khanum, R., Mumtaz, A. S., & Kumar, S. (2013). Predicting impacts of climate change on medicinal asclepiads of Pakistan using Maxent modeling. *Acta Oecologica, 49*, 23–31. https://doi.org/10.1016/j.actao.2013.02.007

KirkSpriggs, A., & Sinclair, B. (2017). *Manual of Afrotropical Diptera. Volume 1. Introductory chapters and keys to Diptera families*. (A. KirkSpriggs & B. Sinclair, Eds.) (pp. 1–67). Pretoria: South African National Biodiversity Institute.

Knutti, R., Furrer, R., Tebaldi, C., Cermak, J., & Meehl, G. A. (2010). Challenges in Combining Projections from Multiple Climate Models. *Journal of Climate, 23*(10), 2739–2758. https://doi.org/10.1175/2009jcli3361.1

Lange, S., Büchner, M., & Langer, S. (2020). ISIMIP3b bias-adjusted atmospheric climate input data (v1.1). ISIMIP Repository. https://doi.org/10.48364/ISIMIP.842396.1

Liu, C., Berry, P. M., Dawson, T. P., & Pearson, R. G. (2005). Selecting thresholds of occurrence in the prediction of species distributions. *Ecography, 28*(3), 385–393. https://doi.org/10.1111/j.0906-7590.2005.03957.x

Liu, C., White, M., & Newell, G. (2011). Measuring and comparing the accuracy of species distribution models with presence-absence data. *Ecography, 34*(2), 232–243. https://doi.org/10.1111/j.1600-0587.2010.06354.x

Longbottom, J., Caminade, C., Gibson, H. S., Weiss, D. J., Torr, S., & Lord, J. S. (2020). Modelling the impact of climate change on the distribution and abundance of tsetse in Northern Zimbabwe. *Parasites & Vectors, 13*(1). https://doi.org/10.1186/s13071-020-04398-3

Longbottom, J., Esterhuizen, J., Hope, A., Lehane, M. J., Mangwiro, T. C., Mugenyi, A., et al. (2024). Impact of a national tsetse control programme to eliminate Gambian sleeping sickness in Uganda: a spatiotemporal modelling study. *BMJ Global Health, 9*(10), e015374–e015374. https://doi.org/10.1136/bmjgh-2024-015374

Lord, J. S., Hargrove, J. W., Torr, S. J., & Vale, G. A. (2018). Climate change and African trypanosomiasis vector populations in Zimbabwe's Zambezi Valley: A mathematical modelling study. *PLOS Medicine, 15*(10), Article e1002675. https://doi.org/10.1371/journal.pmed.1002675

McSweeney, C. F., Jones, R. G., Lee, R. W., & Rowell, D. P. (2015). Selecting CMIP5 GCMs for downscaling over multiple regions. *Climate Dynamics, 44*(11–12), 3237–3260. https://doi.org/10.1007/s00382-014-2418-8

Messina, J. P., Moore, N., DeVisser, M. H., McCord, P., & Walker, E. D. (2012). Climate Change and Risk Projection: Dynamic Spatial Models of Tsetse and African Trypanosomiasis in Kenya. *Annals of The Association of American Geographers, 102*(5), 1038–1048. https://doi.org/10.1080/00045608.2012.671134

Moore, S., Shrestha, S., Tomlinson, K. W., & Vuong, H. (2012). Predicting the effect of climate change on African trypanosomiasis: integrating epidemiology with parasite and vector biology. *Journal of The Royal Society Interface, 9*(70), 817–830. https://doi.org/10.1098/rsif.2011.0654

Morales, N. S., Fernández, I. C., & Baca-González, V. (2017). MaxEnt's parameter configuration and small samples: are we paying attention to recommendations? A systematic review. *PeerJ, 5*. https://doi.org/10.7717/peerj.3093

Mugenyi, A., Muhanguzi, D., Hendrickx, G., Nicolas, G., Waiswa, C., Torr, S., et al. (2021). Spatial analysis of G.f.fuscipes abundance in Uganda using Poisson and Zero-Inflated Poisson regression models. *PLOS Neglected Tropical Diseases, 15*(12), e0009820. https://doi.org/10.1371/journal.pntd.0009820

Muyobela, J., Pirk, C. W. W., Yusuf, A. A., & Sole, C. L. (2023). Spatial distribution of Glossina morsitans (Diptera: Glossinidae) in Zambia: A vehicle-mounted sticky trap survey and Maxent species distribution model. *PLOS Neglected Tropical Diseases, 17*(7), Article e0011512. https://doi.org/10.1371/journal.pntd.0011512

Newstead, R. (1910). On Three New Species of the Genus Glossina, Together with a Description of the Hitherto

Unknown Male ofGlossina Grossa, Bigot. *Annals of Tropical Medicine & Parasitology, 4*(3), 369–375. https://doi.org/10.1080/00034983.1910.11685725

Nnko, H. J., Gwakisa, P. S., Ngonyoka, A., Sindato, C., & Estes, A. B. (2021). Potential impacts of climate change on geographical distribution of three primary vectors of African Trypanosomiasis in Tanzania's Maasai Steppe: G. m. morsitans, G. pallidipes and G. swynnertoni. *PLOS Neglected Tropical Diseases, 15*(2), e0009081.https://doi.org/10.1371/journal.pntd.0009081

O'Neill, B. C., Tebaldi, C., van Vuuren, D. P., Eyring, V., Friedlingstein, P., Hurtt, G., et al. (2016). The Scenario Model Intercomparison Project (ScenarioMIP) for CMIP6. *Geoscientific Model Development, 9*(9), 3461–3482. https://doi.org/10.5194/gmd-9-3461-2016

Pearson, R. G., Raxworthy, C. J., Nakamura, M., & Townsend Peterson, A. (2007). Predicting species distributions from small numbers of occurrence records: a test case using cryptic geckos in Madagascar. *Journal of Biogeography, 34*(1), 102–117. https://doi.org/10.1111/j.1365-2699.2006.01594.x

Peterson, A. T., Papeş, M., & Soberón, J. (2008). Rethinking receiver operating characteristic analysis applications in ecological niche modeling. *Ecological Modelling, 213*(1), 63–72. https://doi.org/10.1016/j.ecolmodel.2007.11.008

Phillips, S. J., Anderson, R. P., & Schapire, R. E. (2006). Maximum entropy modeling of species geographic distributions. *Ecological Modelling, 190*(3–4), 231–259. https://doi.org/10.1016/j.ecolmodel.2005.03.026

Phillips, S. J., Dudík, M., Elith, J., Graham, C. H., Lehmann, A., Leathwick, J., & Ferrier, S. (2009). Sample selection bias and presenceonly distribution models: implications for background and pseudoabsence data. *Ecological Applications, 19*(1), 181–197. https://doi.org/10.1890/072153.1

Phillips, S. J., Dudík, M., & Schapire , R. E. (2024). Maxent software for modeling species niches and distributions (version 3.4.4). https://biodiversityinformatics.amnh.org/open_source/maxent. Accessed 10 August 2024

Riahi, K., van Vuuren, D. P., Kriegler, E., Edmonds, J., O'Neill, B. C., Fujimori, S., et al. (2017). The Shared Socioeconomic Pathways and their energy, land use, and greenhouse gas emissions implications: An overview. *Global Environmental Change, 42*(42), 153–168. https://www.sciencedirect.com/science/article/pii/S0959378016300681

Saarman, N., Burak, M., Opiro, R., Hyseni, C., Echodu, R., Dion, K., et al. (2018). A spatial genetics approach to inform vector control of tsetse flies (*Glossina fuscipes* fuscipes) in Northern Uganda. *Ecology and Evolution, 8*(11), 5336–5354. https://doi.org/10.1002/ece3.4050

Sclater, P. L. (1858). On the general Geographical Distribution of the Members of the Class Aves. *Journal of the proceedings of the Linnean Society, 2*(7), 130–136. https://doi.org/10.1111/j.1096-3642.1858.tb02549.x

Sofaer, H. R., Jarnevich, C. S., Pearse, I. S., Smyth, R. L., Auer, S., Cook, G. L., et al. (2019). Development and Delivery of Species Distribution Models to Inform Decision-Making. *BioScience, 69*(7), 544–557. https://doi.org/10.1093/biosci/biz045

Swets, J. (1988). Measuring the accuracy of diagnostic systems. *Science, 240*(4857), 1285–1293. https://doi.org/10.1126/science.3287615

Wallace , A. R. (1876). *The geographical distribution of animals* (p. 503). London: Mac Millan

Warren, D. L., & Seifert, S. N. (2011). Ecological niche modeling in Maxent: the importance of model complexity and the performance of model selection criteria. *Ecological Applications, 21*(2), 335–342. https://doi.org/10.1890/10-1171.1

Yan, H., He, J., Zhao, Y., Zhang, L., Zhu, C., & Wu, D. (2020). Gentiana macrophylla response to climate change and vulnerability evaluation in China. *Global Ecology and Conservation, 22*, e00948–e00948. https://doi.org/10.1016/j.gecco.2020.e00948

Zhou, R., Gao, Y., Chang, N., Gao, T., Ma, D., Li, C., & Liu, Q. (2021). Projecting the potential distribution of glossina morsitans (diptera: glossinidae) under climate change using the MaxEnt model. *Biology, 10*(11), 1150. https://doi.org/10.3390/biology10111150